# Chapter 4
# High Penetration of Rooftop Photovoltaic Cells in Low Voltage Distribution Networks: Voltage Imbalance and Improvement

**Farhad Shahnia and Arindam Ghosh**

**Abstract** Installation of domestic rooftop photovoltaic cells (PVs) is increasing due to feed–in tariff and motivation driven by environmental concerns. Even though the increase in the PV installation is gradual, their locations and ratings are often random. Therefore, such single–phase bi–directional power flow caused by the residential customers can have adverse effect on the voltage imbalance of a three–phase distribution network. In this chapter, a voltage imbalance sensitivity analysis and stochastic evaluation are carried out based on the ratings and locations of single–phase grid–connected rooftop PVs in a residential low voltage distribution network. The stochastic evaluation, based on Monte Carlo method, predicts a failure index of non–standard voltage imbalance in the network in presence of PVs. Later, the application of series and parallel custom power devices are investigated to improve voltage imbalance problem in these feeders. In this regard, first, the effectiveness of these two custom power devices is demonstrated vis–à–vis the voltage imbalance reduction in feeders containing rooftop PVs. Their effectiveness is investigated from the installation location and rating points of view. Later, a Monte Carlo based stochastic analysis is utilized to investigate their efficacy for different uncertainties of load and PV rating and location in the network. This is followed by demonstrating the dynamic feasibility and stability issues of applying these devices in the network.

F. Shahnia (✉)
Center of Smart Grid and Sustainable Power Systems,
Department of Electrical and Computer Engineering,
Curtin University, Perth, Australia
e-mail: farhad.shahnia@curtin.edu.au

A. Ghosh
School of Electrical Engineering & Computer Science,
Queensland University of Technology, Brisbane, Australia
e-mail: a.ghosh@qut.edu.au

J. Hossain and A. Mahmud (eds.), *Renewable Energy Integration*,
Green Energy and Technology, DOI: 10.1007/978-981-4585-27-9_4,

**Keywords** Distribution network · Single–phase rooftop PV · Voltage imbalance · Sensitivity analysis · Stochastic evaluation · DSTATCOM · DVR

## 4.1 Introduction

Current and voltage imbalance is one of the major power quality problems in low voltage distribution networks [1]. Voltage imbalance is more common in individual customer loads due to phase load imbalances, especially where large single–phase power loads are used [2]. Although voltages are well balanced at the supply side, the voltages at the customer level can become unbalanced due to the unequal system impedances, unequal distribution of single–phase loads or large number of single–phase transformers [2]. Usually, the electric utilities aim to distribute the residential loads equally among the three phases of distribution feeders [3].

An increase in the voltage imbalance can result in overheating and de-rating of all induction motor types of loads [4]. Voltage imbalance can also cause network problems such as mal-operation of protection relays and voltage regulation equipment, and generation of non–characteristic harmonics from power electronic loads [3].

In recent years, there is a growing interest in the residential customers in installing of single-phase grid-connected rooftop Photovoltaic cells (PVs) due to new energy and incentive polices in several countries [5]. The most important characteristic of these PVs is that their output power being fed to the grid is not controlled and is dependent on the instantaneous power from the sun. Several technical problems of these systems such as harmonics, voltage profile and power losses are already studied and investigated in [6–8].

The residential rooftop PVs are currently installed randomly across distribution systems. This may lead to an increase in the imbalance index of the network [9]. This will increasingly cause problems for three-phase loads (e.g. motors for pumps and elevators). Therefore, there is a need for investigating the sensitivity analysis of voltage imbalance in these networks.

A deterministic analysis may not be suitable due to the randomness of PV installations and their intermittent nature of power generation. Monte Carlo method is already applied for analysis of uncertainties in the network in order to study load flow, voltage sag, fault and reliability [10]. Therefore, a stochastic evaluation based on Monte Carlo method is carried out in this chapter to investigate and predict the network voltage imbalance for the uncertainties arising due to rooftop PV power ratings and locations [11].

Some voltage imbalance improvement methods are already proposed and investigated in [12–14]. However, parallel and series converter–based Custom Power Devices (CPD) can also be used for power quality improvement [1, 15]. In this chapter, the application of CPDs, in particular, Distribution Static Compensator

(DSTATCOM) and Dynamic Voltage Restorer (DVR) are demonstrated for voltage imbalance reduction and voltage profile correction within these networks. Their optimum installation location, efficacy and ratings will be discussed. However, due to uncertainty in load demand and PV generation in addition to PV ratings and locations along the feeder, a Monte Carlo based stochastic analysis is carried out later to investigate the efficacy of the proposed CPDs for many different uncertainties within the network. Finally, the dynamic feasibility of the system in the presence of the proposed improvement methods will be demonstrated.

## 4.2 Voltage Imbalance in Low Voltage Distribution Networks

The Electricity supplies are nominally 110 V (in US and Canada) or 220–240 V. National standards specify that the nominal voltage at the source should be in a narrow tolerance range. Based on Australian Standard Voltages, AS60038–2000, Australian low voltage network is 230 V with a tolerance between +10 % and −6 % [16].

Voltage imbalance in three–phase systems is a condition in which the three phase voltages differ in magnitude and/or do not have normal 120° phase differences. IEEE Recommended Practice for Monitoring Electric Power Quality defines voltage imbalance as [17]

$$VUF\,\% = \left|\frac{V_-}{V_+}\right| \times 100 \tag{4.1}$$

where $V_-$ and $V_+$ are the negative and positive sequence of the voltage, respectively. This will be referred to as percentage voltage imbalance in the chapter. According to [17], the allowable limit for voltage imbalance is limited to 2 % in low voltage networks. Engineering Recommendation P29 in UK not only limits voltage imbalance of the network to 2 %, but also limits the voltage imbalance to 1.3 % at the load point [18]. In this chapter, we assume that the standard limit is 2 %.

The utilities try to minimize the imbalance index in their network by distributing single–phase loads equally across all three phases. Probabilistic studies have shown that it is very rare that the residential and small business loads can result in higher values of the voltage imbalance in the network. The measurements done in a low voltage distribution network in US [19], Brazil [20] and Iran [21] conclude that the probability of the voltage imbalance to be more than 3 % in the network is about 2–5 %. However, this can only be achieved if the engineering judgements have been applied for selecting the appropriate size of the conductors and cables, transformer ratings and also if the load dispatch among the three phases are recorrected by later observations and measurements. If the appropriate designs have not been done or there is a non–standard voltage drop in the network, it is highly probable that the network also suffers from higher voltage imbalance.

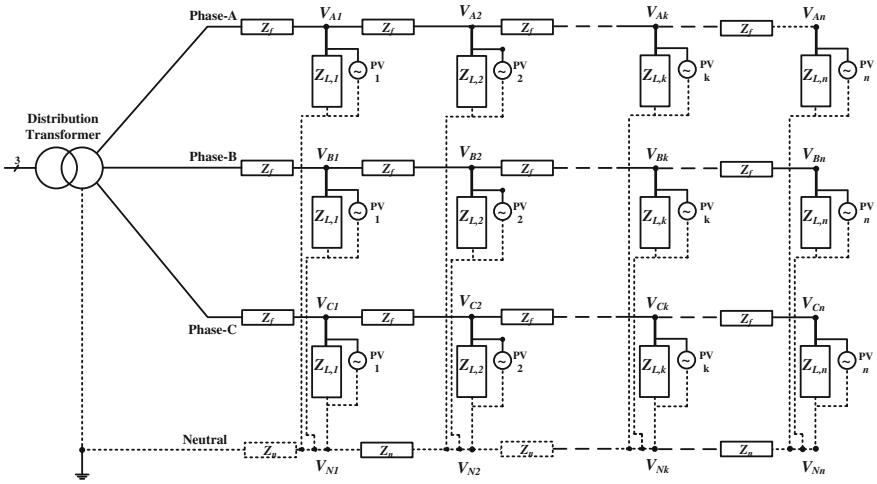


**Fig. 4.1** Schematic single line diagram of the considered low voltage distribution network

As mentioned before, rooftop PVs that are currently being installed depend on outlook and financial condition of householders. Therefore, it is not unexpected that these installations are randomly placed along distribution feeders. For example, it is possible that 80 % of customers on a phase have installed PVs, while the other two phases have only 50 and 10 % installed. In such a condition, even if the voltage imbalance of the network was within the standard limits without any PVs, it is not guaranteed to remain so. Therefore, the possible PV installation number or rating on such systems must be investigated in a way that the voltage imbalance is still kept within the standard limit.

### *4.2.1 Network Structure*

A sample radial low voltage residential urban distribution network is considered for voltage imbalance investigations. The simplified equivalent single line diagram of one feeder of the network is illustrated in Fig. 4.1. In this model, the PVs are all grid–connected such that the surplus of the electricity generated will flow to the grid. It has been assumed that all the PVs work at unity power factor based on IEEE Recommended Practice for Utility Interface of Photovoltaic Systems [22]. It is also assumed that the neutral conductor is making the path for unbalance current circulation and the analysis is based on the mutual effect of three phases.

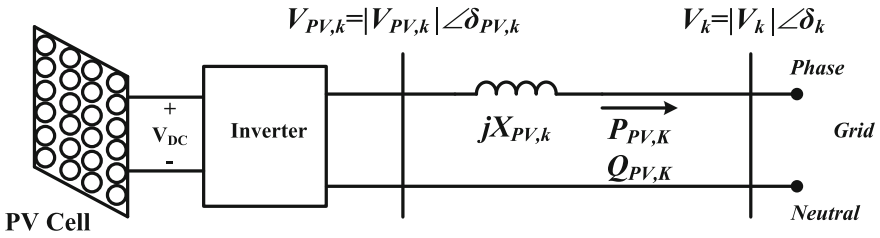


**Fig. 4.2** Schematic diagram of a PV connection to grid

### 4.2.2 Power Flow Analysis

For calculating the voltage imbalance, it is necessary that the network to be analysed and the voltages at the desired nodes to be calculated. Based on the KCL on $k$th node of phase $A$, we have

$$\frac{\beta\left(V_{A,PV,k}-V_{A,k}\right)}{X_{A,PV,k}}+\frac{V_{A,k-1}-V_{A,k}}{Z_f}+\frac{V_{A,k+1}-V_{A,k}}{Z_f}+\frac{V_{N,k}-V_{A,k}}{Z_{A,L,k}}=0 \tag{4.2}$$

where $Z_f$ is the feeder impedance between two adjacent nodes in phase lines, $V_{A,i,}$ $i=1,\ldots,n$ is the single–phase voltage of the $i$th node of phase $A$, $Z_{A,L,k}$ is the load impedance connected to $k$th node of phase $A$ and and $V_{N,k}$ is the voltage of the neutral wire connected to $k$th node. $V_{A,PV,k}$ and $X_{A,PV,k}$ are the PV voltage and impedance connected to $k$th node of phase $A$. Similar equations are valid for phases $B$ and $C$. In (4.2), the controlling constant $\beta$ is equal to 1 when there is a PV connected to $k$th node, otherwise, it is zero.

KCL for each node on the neutral line is

$$\frac{V_{N,k-1}-V_{N,k}}{Z_n}+\frac{V_{N,k+1}-V_{N,k}}{Z_n}+\frac{V_{N,k}-V_{A,k}}{Z_{A,L,k}}+\frac{V_{N,k}-V_{B,k}}{Z_{B,L,k}}+\frac{V_{N,k}-V_{C,k}}{Z_{C,L,k}}=0 \tag{4.3}$$

where $Z_n$ is the feeder impedance between two adjacent nodes in neutral line.

The simplified diagram of the PV connection to the grid is shown in Fig. 4.2. Based on this figure, we have

$$P_{PV,k}=\frac{\left|V_{PV,k}\right|\left|V_k\right|}{X_{PV,k}}\sin\left(\delta_{PV,k}-\delta_k\right) \tag{4.4}$$

$$Q_{PV,k}=\frac{|V_k|}{X_{PV,k}}\left(\left|V_{PV,k}\right|\cos\left(\delta_{PV,k}-\delta_k\right)-|V_k|\right) \tag{4.5}$$

where $P_{PV,k}$ and $Q_{PV,k}$ are respectively the active and reactive power output of the PV connected to $k$th node. Assuming $P_{PV,k}$ and $Q_{PV,k}$ to be constant and $|V_k|$ and $\delta_k$ are known, $|V_{PV,k}|$ and $\delta_{PV,k}$ can be calculated. Please note that $Q_{PV,k}$ will be zero if the PV operates in Unity Power Factor (UPF).

To calculate $V_k$ from (4.2)–(4.5), an iterative method is required. Starting with a set of initial values, the entire network is solved to determine $V_k$. Once the solution converges, the sequence components are calculated. These sequence components are later used to voltage imbalance calculation given in (4.1).

### 4.2.3 Sensitivity Analysis

The voltage at any node can be considered as a function of the location and rating of PV. Therefore the sensitivity of network voltage imbalance to a PV location and rating is expressed as

$$S_k = \frac{\partial VUF}{\partial P_{PV,k}} \cdot \frac{P_{PV,k}}{VUF} \tag{4.6}$$

Since voltages at each node are calculated iteratively, the sensitivity is calculated numerically once the iterations converge as

$$S_k = \frac{VUF(\gamma+1) - VUF(\gamma)}{P_{PV,k}(\gamma+1) - P_{PV,k}(\gamma)} \tag{4.7}$$

where $0 \leq \gamma \leq 4$ defines the rating of the PV (i.e. 0, 1, 2, 3, 4, 5 kW).

### 4.2.4 Stochastic Evaluation

Monte Carlo simulation is a powerful numerical method of stochastic evaluation based on random input variables [17].

The inherent characteristic of low voltage distribution networks includes random variation of residential load demand and PV power generation at different time periods. This variation is based on load demand in about 12 h sunshine daily pattern and summer–winter periods. In addition to this, the random location and nominal power of PVs increase the randomness of the network.

For investigating the voltage imbalance in the network when there is a random combination of rooftop PVs with different ratings and at different location on all phases and feeders on the network, a stochastic evaluation based on Monte Carlo method has been carried out. Three random inputs of the stochastic evaluation are the number of householders with installed rooftop PVs, the ratings of the PVs and their location in the different phases and feeders. The flowchart of Monte Carlo method is shown in Fig. 4.3. In this figure, the inputs are network (load, feeder and transformer) data. The random number generation and selection of the other parameters for the Monte Carlo method is explained in Sect. 4.3.2. For each set of data, the load flow is carried out and voltage imbalance is calculated.

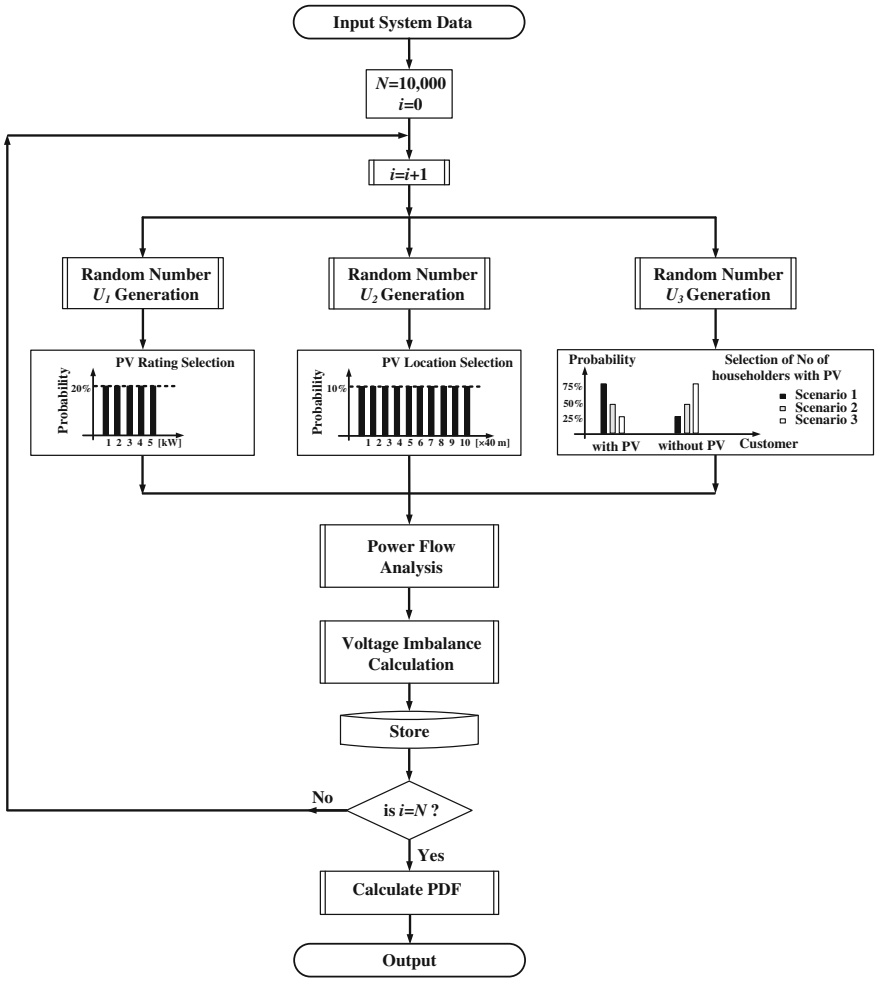


**Fig. 4.3** Monte Carlo flowchart for stochastic evaluation

The expected voltage imbalance at the calculation node $\overline{VUF}_j$ from each trial $1 \leq k \leq N$, is calculated by

$$\overline{VUF}_j = \frac{1}{N} \sum_{k=1}^{N} VUF_k \tag{4.8}$$

The unbiased sample variance for voltage imbalance at the calculated nodes (beginning or end of feeder) is as follows:

$$Var(VUF_j) = \frac{1}{N-1}\sum_{k=1}^{N}\left(VUF_k - \overline{VUF_j}\right)^2 \tag{4.9}$$

The stopping rule of the Monte Carlo method is chosen based on achieving an acceptable convergence for $\overline{VUF}$ and *Var(VUF)*. In this study, the number of Monte Carlo trials is chosen as N = 10,000 to achieve an acceptable convergence. This is more explained in the table in Appendix A.

The voltage imbalance results as the output of the Monte Carlo simulations are used to calculate the Probability Density Function (PDF) and the average (mean value) of all voltage imbalances which is shown as $\lambda$ in the chapter.

## 4.3 Sensitivity and Stochastic Analysis Results

A sample radial low voltage (415 V) residential urban distribution network is considered for voltage imbalance investigations. This network is supposed to supply electricity to a combination of residential and small business customers. It has three feeders, each three-phase and 4-wire system with equal length (400 m) and equal number of customers on each phase and feeder. The poles are located at a distance of almost 40 m from each other. At each pole, 2 houses are supplied from each phase. The feeders and their cross–section are also designed appropriately based on the amount of power and the voltage drop. The technical data of the network is given in the Appendix B.

It is assumed that the total electric demand of the network is almost 1 MVA including the low voltage network under consideration that is supplying a total demand of 360 kW. It is also assumed that during the period of study the loads of phase *A*, *B* and *C* are 60, 120 and 180 kW, respectively. The rest of the network load (the portion not included in this study) is considered as a lumped load. The rooftop PVs installed by the householders have an output power in the range of 1–5 kW working in unity power factor. Several studies are performed [11] and their results are discussed below.

The utilities usually measure and monitor the voltage imbalance at the beginning of the feeder (i.e. secondary side of the distribution transformer). As described previously, the probabilistic studies of the measurement results show that there is low chance of having a voltage imbalance beyond 2 % at this location. Let us assume that the length of the three phases and number of customers per phase are the same. Even then, since the power consumption of the loads are different, there will be different voltage drops along the feeder. This will result in different voltage amplitudes and angles at different locations along the feeder. This phenomenon can result in high voltage imbalance especially at the end of the feeders. To keep the voltage drop within the limit all along the feeder, the utilities install single–phase pole mounted capacitors or increase the cross–section of the feeder. However, voltage imbalance at the end of the feeder still remains higher

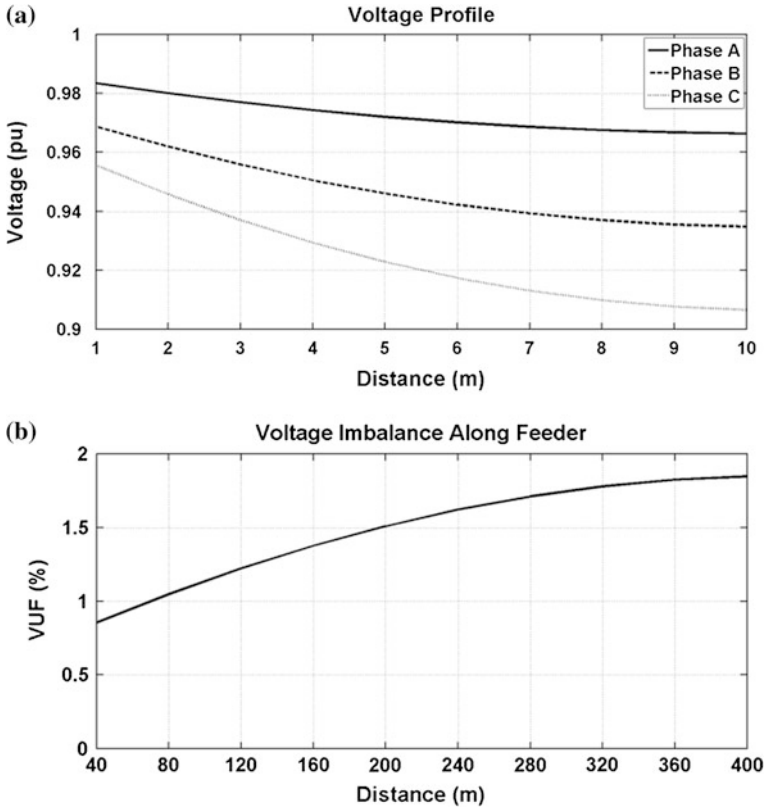


**Fig. 4.4** **a** Network voltage profile along the feeder, **b** Voltage imbalance profile along the feeder

than the beginning of the feeder. This might cause a problem if some three–phase induction motors or power electronics based equipment are located far from the beginning of the feeder. The voltage profile and voltage unbalance profile along the feeder in the system under consideration is shown in Figs. 4.4a and b, respectively. From this figure, it can be seen that the voltage amplitude at the beginning of the feeder is 0.98, 0.96 and 0.95 pu for phases *A*, *B* and *C* respectively. These values are decreased to 0.96, 0.93 and 0.90 pu at the end of the feeder, respectively. Therefore, voltage imbalance at the beginning of the feeder has increased from 0.85 to 1.84 % at the end.

Due to time varying characteristic of residential load demand and PV output power, a study is included to investigate the voltage imbalance variation during a specific time period. Let us assume some PVs with the power output profile as shown in Fig. 4.5a and the residential loads with load profile as shown in Fig. 4.5b are considered [23, 24]. Time varying characteristic of voltage imbalance at the beginning and end of the feeder is shown in Fig. 4.5c. Voltage imbalance has a time varying characteristic and it may increase depending on the PVs.

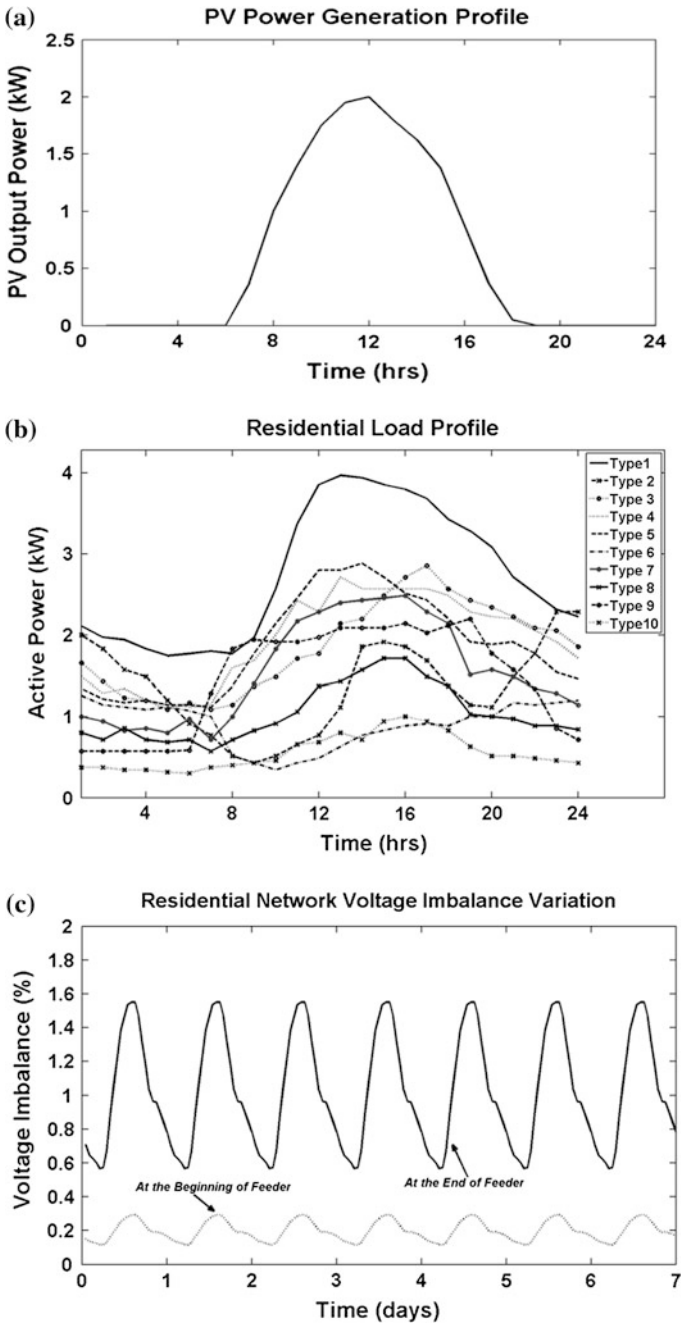


**Fig. 4.5** **a** Power generation profile of a 2 kW rooftop PV, **b** 10 different types of residential loads profiles, **c** Time varying characteristic of voltage imbalance with constant location for PVs in the network

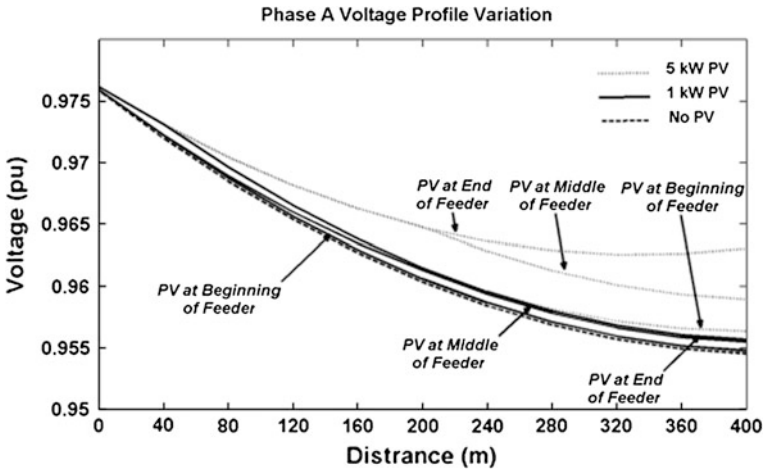


**Fig. 4.6** Variation of phase *A* voltage profile versus the location and rating of the PV in phase *A*

### *4.3.1 Sensitivity Analysis of a Single PV on Voltage Imbalance*

The voltage imbalance variation due to the location of one PV with a constant rating will depend on the total load of the phase in which it is installed. Usually rooftop PVs can have ratings up to 5 kW for urban residential customers. It is also important to define the point at which the voltage imbalance will be measured.

It is expected that the voltage profile will improve in the phase the PV is installed. Let us consider either a 1 or a 5 kW PV installation at the beginning, middle and end of a feeder. In Fig. 4.6, the voltage profile of phase *A* is shown. As expected, the voltage amplitude increases with PV of higher ratings or when it is installed at the end.

The installation of a PV in a low load phase (phase *A* in this case) results in the increase in voltage difference and hence voltage imbalance at the end of the feeder while having minor effect at the beginning of the feeder. This voltage imbalance is more if the PV is installed at the end of the feeder or if the rating of the PV is high. The sensitivity analysis of voltage imbalance (calculated at the end of the feeder) versus the location and rating of rooftop PV installed in low load phase *A* is shown in Fig. 4.7a.

The voltage difference between the phases reduces if the PV is installed in high load phase (phase *C*). The decrease is more pronounced at the end of the feeder than at the beginning. This decrease at the end of the feeder is more if the PV is installed at the end of the feeder or if the rating of the PV is high. The sensitivity analysis of voltage imbalance (calculated at the end of the feeder) versus the location and rating of rooftop PV installed in high load phase *C* is illustrated in Fig. 4.7b.

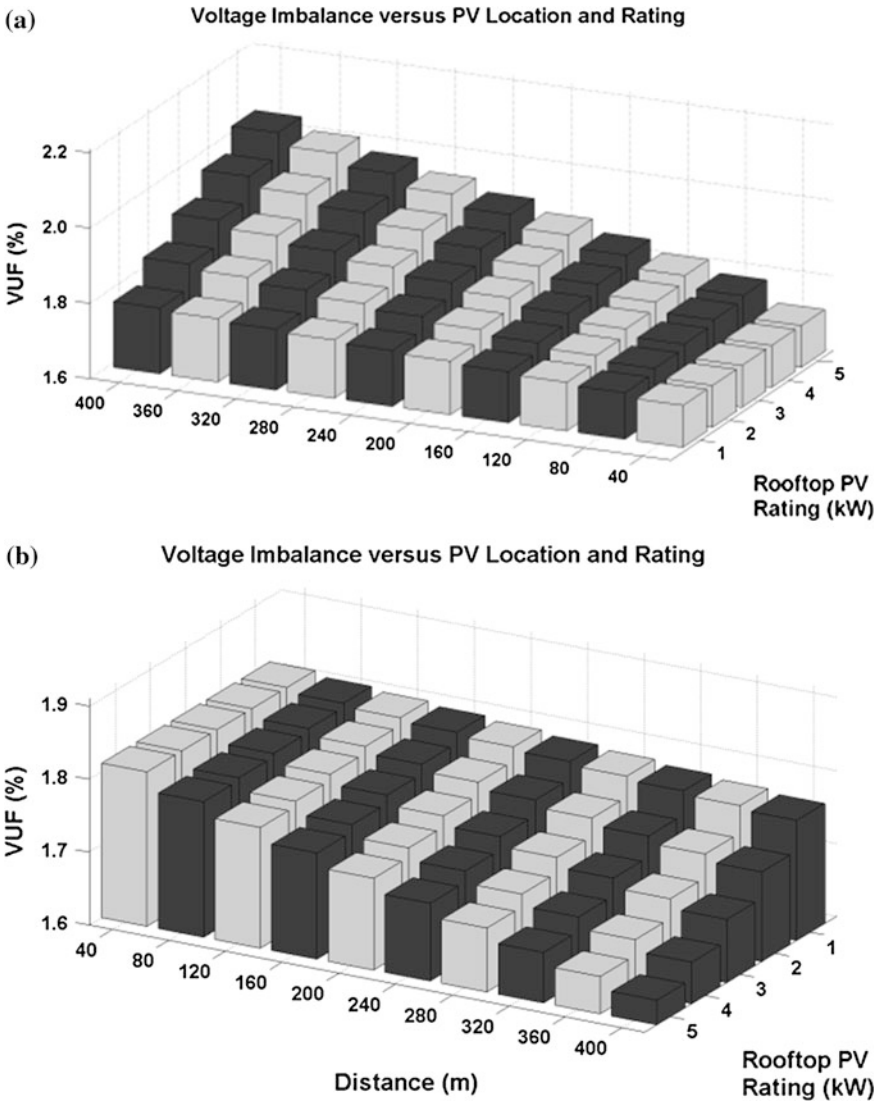


**Fig. 4.7** Voltage imbalance sensitivity analysis versus PV location and rating in **a** low load phase—Phase *A*, **b** high load phase—Phase *C*

These results prove that a rooftop PV (with a rating of less than 5 kW) can cause network voltage imbalance to increase by 0.1 % when installed at the beginning of the feeder and by 25 % when installed at the end of the feeder, specifically when the feeder supplies up to 1 MW load. For example, in the worst case, the voltage imbalance of 1.84 % without any PV increased to 2.02 % (i.e., a 25 % rise) when a 5 kW PV was installed at the end of the feeder. Even in this

worst case, the voltage imbalance, at the end of the feeder, is not significant since it still does not lead to non-standard voltage imbalance. However, this may not be true when more than one PV get installed in the network.

### 4.3.2 Stochastic Evaluation of Voltage Imbalance

A stochastic evaluation is carried out for investigating the uncertainties in the network [11]. In this study, it is assumed the PVs (with rating of 1, 2, 3, 4, 5 kW) have equal probability of 20 % each, as shown in Fig. 4.3. The uncertainty in the PV rating is modelled by drawing a random number $U_1$ distributed uniformly under [0, 1]. Using $U_1$, the instantaneous output power of each PV is selected in 0–5 kW range during day–night period. The uncertainty of PV location along the feeder, [0–400 m], is modelled by drawing a random number $U_2$ distributed uniformly under [0, 1]. This is done for all phases and feeders of the studied network independently.

The number of the householders with installed rooftop PVs is assumed to be ¼, ½ and ¾ of the total number of householders as 3 different scenarios, shown in Fig. 4.3. For selecting 1 out of these 3 scenarios, a random number $U_3$ distributed uniformly under [0, 1] is used. If $U_3 < 0.33$ then scenario 1 is selected, if $0.33 \leq U_3 \leq 0.66$ then scenario 2 is selected and if $U_3 > 0.66$ then scenario 3 is selected.

Another study was also carried out with normal distributions for $U_1$ with ($\mu = 0.5$ and $\sigma = 0.2$) and also $U_3$ with ($\mu = 0.3$ and $\sigma = 0.08$) that due to similarity in the results are not shown here.

This study was carried out for several times with minimum number of N = 10,000 trials. A sample result for the scenario of ½ householders having PV are shown in Fig. 4.8a. It can be seen that the voltage imbalance calculated at the beginning of the feeder always remain about 0.8 %. This value for the end of the feeder varies between 1 and 3 %.

The PDFs for the cases when ½ of the householders have PVs is shown in Fig. 4.8b. The PDFs for all the three cases have mean value ($\lambda$) equal to 0.61 % at the beginning of the feeder and 1.80 % at the end of the feeder.

From Fig. 4.8b, it can be seen that, there is a high probability that the voltage imbalance at the end of the feeder is more than the 2 % standard limit. This probability is referred to as the failure index ($F_I$ %) which is the frequency of the cases in the shaded area in probability density function and is calculated as

$$F_I\% = shaded\,area \times 100 \tag{4.10}$$

While voltage imbalance failure index is zero at the beginning of the feeder, it is about 30.19 % at the end of the feeder.

The customer load consumption is different at different times. Therefore, the residential loads also have an effect on the voltage imbalance. This phenomenon is

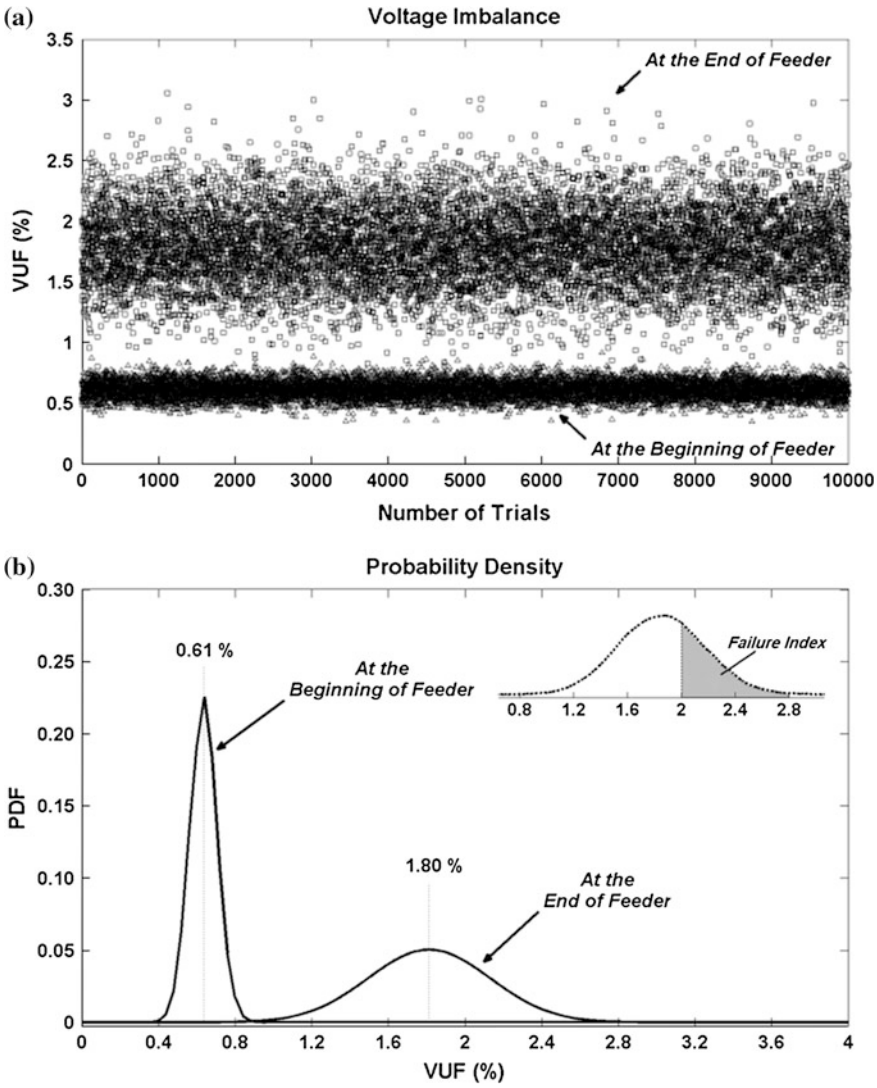


**Fig. 4.8** **a** Voltage imbalance for 10,000 scenarios of random location and ratings of PVs. **b** Probability density function of voltage imbalance

included as the fourth uncertainty condition for Monte Carlo method. The results of this analysis are given in Table 4.1 for different load consumption levels in the network during different times. It can be seen that when the loads are almost balanced, $\lambda$ and failure index decrease while they increase if the loads are highly unbalanced.

**Table 4.1** $\lambda$ and failure indices of voltage imbalance of the studied low voltage distribution network for different residential load levels

| Residential load status | Highly unbalanced | Lightly unbalanced | Almost balanced |
|---|---|---|---|
| $\lambda$ at beginning of feeder | 0.66 | 0.58 | 0.46 |
| $\lambda$ at end of feeder | 1.92 | 1.70 | 1.37 |
| Failure index ($F_I$ %) | 46.0 | 22.3 | 6.0 |

**Table 4.2** $\lambda$ and failure indices of voltage imbalance of the studied network considering majority of pvs installed at beginning or end of the feeder

| Majority of PVs installed at | Beginning of feeder | Middle of feeder | End of feeder |
|---|---|---|---|
| $\lambda$ at beginning of feeder | 0.61 | 0.61 | 0.62 |
| $\lambda$ at end of feeder | 1.88 | 1.97 | 2.06 |
| Failure Index ($F_I$ %) | 16.2 | 51.8 | 67.9 |

The influence of the location of the PVs (at the beginning or end of the feeder) on voltage imbalance is discussed before. In the previous studies, it was assumed the PVs are distributed randomly along the feeder. It is of high interest to investigate the case when the majority of the PVs are installed at the beginning or at the end of the feeder. Therefore, another Monte Carlo study is carried out to investigate this phenomenon. The results of this study given are in Table 4.2. It can be seen that generally when the majority of the PVs are installed at the end of the feeder, the failure index and $\lambda$ increase at the end points of the network.

## 4.4 Voltage Imbalance Improvement using Custom Power Devices

In this section, the series and parallel custom power devices are applied to fix the voltage at Point of Common Coupling (PCC) by forcing the three phase voltages magnitudes to be the same as desired, while their phases are separated by 120° [25].

### *4.4.1 DSTATCOM*

A DSTATCOM is connected in parallel to the network, as shown in Fig. 4.9a. It will fix the voltage magnitude at PCC to desired value of $0.94 \leq E_{DSTAT} \leq 1$ pu by injecting/absorbing a required amount of reactive power. Hence the DSTATCOM can be supplied by only a DC capacitor.

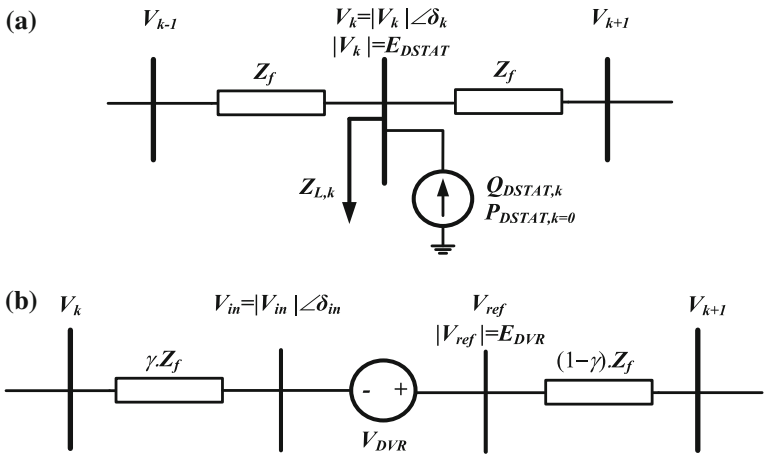


**Fig. 4.9** **a** Single line diagram of DSTATCOM connection, **b** Single line diagram of DVR connection

Let us assume that a three–phase DSTATCOM is installed at the *k*th node, which will be assumed to be a voltage controlled node (i.e., with constant active power and voltage magnitude). The sum of active power injected by DSTATCOM in three phases is set to be zero ($P_{DSTAT,k} = 0$) and the voltage magnitude for all three phases is set to be $E_{DSTAT}$.

The amount of reactive power to be injected/absorbed by DSTATCOM is

$$Q_{DSTAT,k} = -\mathrm{Im}\left\{V_k^* \times \left[\left(V_k \times \left(\frac{2}{Z_f} + \frac{1}{Z_{L,k}}\right)\right) + \left(\frac{V_{k-1} + V_{k+1}}{Z_f} + \frac{V_{N,k}}{Z_{L,k}}\right)\right]\right\} \tag{4.11}$$

Based on the calculated $Q_{DSTAT,k}$, PCC voltage ($V_k$) will be modified as

$$V_k = \frac{1}{\frac{2}{Z_f} + \frac{1}{Z_{L,k}}}\left[\frac{P_{DSTAT,k} - jQ_{DSTAT,k}}{V_k^*} - \left(\frac{V_{k-1} + V_{k+1}}{Z_f} + \frac{V_{N,k}}{Z_{L,k}}\right)\right] \tag{4.12}$$

Equations (4.11)–(4.12) are used in the network analysis iterative method along with equations (4.2)–(4.5) for the node in which the DSTATCOM is installed.

When a DSTATCOM is installed in a node, it will inject/absorb reactive power to fix the voltage in that node to the desired value. By changing the PCC voltage, the voltages of all the nodes will be improved.

### *4.4.2 DVR*

A DVR is connected in series within the network as shown in Fig. 4.9b, where the DVR buses are indicated with voltages of $V_{in}$ and $V_{ref}$. The DVR adds/subtracts a

small amount of voltage in series such that the voltage magnitude such that the magnitude of $V_{ref}$ is equal to a desired value $0.94 \leq E_{DVR} \leq 1$ pu. In Fig. 4.9b, $0 \leq \gamma \leq 1$ represents the location of DVR between two adjacent buses $k$ and $k+1$. Unlike a DSTATCOM, a DVR needs to inject/absorb both active and reactive power. However, as will be shown later, its rating is much smaller than that of a DSTATCOM for the same network.

The amount of necessary voltage to be added by the DVR to phase–$A$ of the network is

$$V_{DVR,A} = V_{ref,A} - V_{in,A} \tag{4.13}$$

The desired voltages at the output of DVR for all three phases are based on same desired magnitude ($E_{DVR}$) and are displaced 120° from each other. These reference voltages are set based on the angle of one of the phases of the voltage $V_{in}$ as

$$\begin{aligned} V_{ref,A} &= E_{DVR}\angle\delta_{in,A} \\ V_{ref,B} &= E_{DVR}\angle\left(\delta_{in,A} - 2\pi/3\right) \\ V_{ref,C} &= E_{DVR}\angle\left(\delta_{in,A} + 2\pi/3\right) \end{aligned} \tag{4.14}$$

The selection of $E_{DVR}$ is based on the location of the DVR along the feeder and will have a significant effect on the rating of the DVR. To optimize the rating while satisfying the voltage and voltage imbalance conditions, $E_{DVR}$ needs to have a higher value if the DVR is installed close to the beginning of feeder and have a lower value if it is installed at far end of the feeder. For network analysis, (4.13) is used in the iterative method of equations (4.2)–(4.5) at the DVR connection point. Unlike a DSTSTCOM, which improves the voltages of all nodes, a DVR installation will improve the voltages of all the nodes downstream of the DVR.

## 4.5 Application of CPDs: Steady–State Results

Let us consider one 11 kV overhead line is feeding several 11 kV/415 V distribution transformers. Only one radial low voltage (415 V) residential feeder is considered with a total load demand of 120 kW. The feeder length is taken as 400 meters. The poles are located at a distance of 40 meters from each other. At each pole, 2 houses are supplied from each phase. The feeders and their cross–section are also designed appropriately based on the nominal power drawn and voltage drop. The technical data of the network is given in Table B.1. in the Appendix B.

It is assumed that during the period of study, the loads of phase $A$, $B$ and $C$ are 20, 40 and 60 kW, respectively. Other distribution transformers with their loads in the 11 kV network are considered as one single lumped load. The rooftop PVs installed by the householders have an output power in the range of 1–5 kW working in UPF. Several studies are performed [25, 26], some of which are discussed below.

### 4.5.1 Nominal Case

Let us first assume there is no rooftop PV installed in the network. The voltage magnitude at the beginning of the feeder is 0.98, 0.97 and 0.97 pu for phases *A*, *B* and *C*, respectively. However, these values decrease to 0.96, 0.94 and 0.92 pu, respectively, at the end of the feeder. Voltage imbalance along the feeder has increased from 0.32 % at the beginning of feeder to 1.31 % at the end.

Let us now consider the case in which rooftop PVs are installed in such a way that very high voltage imbalance results at the end of the feeder. For this purpose, the total power generation of rooftop PVs are assumed to be 40, 5 and 1 kW in phases *A*, *B* and *C*, respectively. Each PV location and rating is given in Table B.1 in the Appendix B. Now, in phase *A*, the power generation of PVs is 40 kW while the load demand is 20 kW. This results in reverse active power flow in phase *A* from PVs to the transformer. Therefore, the voltage profile of phase *A* increases from the beginning of the feeder to the end of the feeder. Hence, voltage imbalance profile along the feeder increases to 2.56 % at the end of the feeder due to unequal distribution of PVs in the network.

### 4.5.2 DSTATCOM Application

Now, let us now assume a DSTATCOM is installed at 280 m (2/3rd) from the beginning of the feeder. The DSTATCOM is controlled to fix the PCC voltage magnitude to $E_{DSTAT} = 0.98$ pu. The voltage profile of the three phases of the network before and after DSTATCOM installation is shown in Fig. 4.10a. In this figure, the dashed lines show the voltage profile when there was no DSTATCOM installed, while the solid lines show that with the DSTATCOM installed. It is clearly evident that the DSTATCOM is capable of fixing the magnitude of all three phases to $E_{DSTAT}$ by injecting reactive power to phases *B* and *C* and absorbing reactive power from phase *A*. In this case, the DSTATCOM has a rating of 80 kVA.

For investigating the effect of DSTATCOM location in voltage imbalance reduction, another study is carried out [26]. In this study, the DSTATCOM is installed in different nodes along the feeder and the voltage imbalance profiles are compared. In Fig. 4.10b, voltage imbalance profile along the feeder is shown before and after DSTATCOM installation in 4 different locations along the feeder: at 1/3rd of feeder from the transformer, midpoint, 2/3rd of feeder and at the end. Comparing the voltage imbalance profiles for these four cases, it can be concluded that DSTATCOM installation is not effective near the beginning of the feeder. Also, when the DSTATCOM is installed exactly at the end of the feeder, the nodes around the midpoint can suffer from higher voltage imbalance values. While if the DSTATCOM is installed somewhere around 2/3rd of feeder, it will have the best result all along the feeder. From this figure, it can be concluded that DSTATCOM will have better results when installed anywhere between the midpoint and 2/3rd of the feeder. Maximum value of voltage imbalance in the network after DSTATCOM

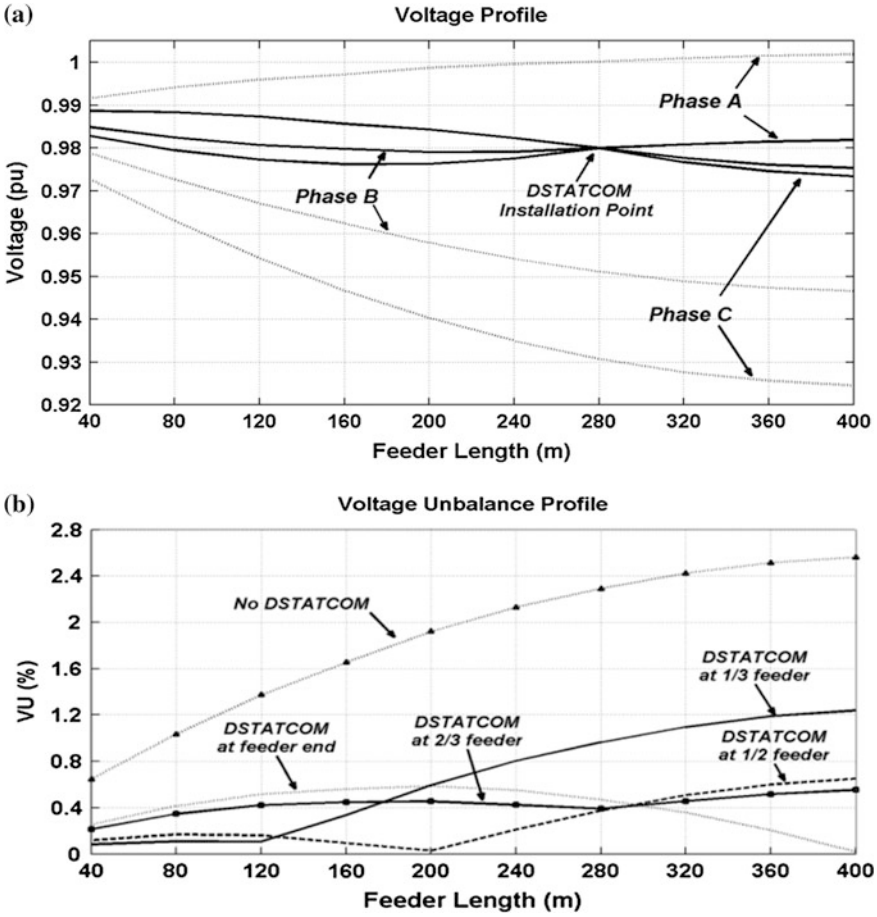


**Fig. 4.10** **a** Low voltage feeder voltage profile before and after DSTATCOM installation at 2/3 of feeder beginning, **b** Low voltage feeder voltage imbalance profile before and after DSTATCOM installation in four different locations along the feeder

installation at 2/3rd of the feeder is 0.55 %, calculated at the end of the feeder. This value is even smaller than the case when no PVs were installed in the network. This verifies the high effectiveness of DSTATCOM application for voltage imbalance reduction and voltage profile improvement in these networks.

### *4.5.3 DVR Application*

Instead of a DSTATCOM, let us now assume a DVR is installed in series with the low voltage feeder, at 120 m (1/3rd) from the feeder beginning. The DVR is applied to fix its output voltage ($V_{ref}$) magnitude to $E_{DVR} = 0.975$ pu. For this case, the DVR will add some positive voltage to phases *B* and *C* and some negative voltage to phase *A*.

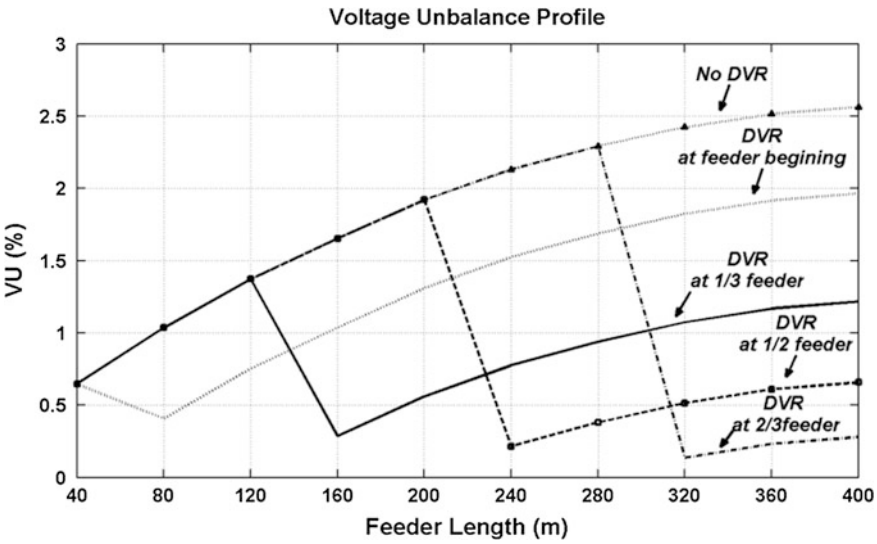


**Fig. 4.11** Low voltage feeder voltage imbalance profile before and after DVR installation in four different locations along the feeder

For investigating the effect of DVR installation and its location in voltage imbalance reduction, another study is carried out [25]. In this study, the DVR is installed in different locations along the feeder and the voltage imbalance profiles are compared. In Fig. 4.11, voltage imbalance profile along the feeder is shown when the DVR is installed in series at very beginning, 1/3rd of feeder, middle and 2/3rd of feeder. Comparing the voltage imbalance profiles for these four cases, it can be concluded that DVR installation is not effective at the very beginning or far end of the feeder. Also, when the DVR is installed exactly at the middle of the feeder, there is a high value of voltage imbalance in the middle of feeder (DVR input side). However, when the DVR is installed at 1/3rd of feeder beginning, voltage imbalance value is smaller all along the feeder compared to other locations. Maximum value of voltage imbalance in the network after DVR installation at 1/3rd of feeder is 1.21 %, calculated at the end of the feeder. Although DVR has reduced voltage imbalance even at the end of the feeder; it is not as successful as DSTATCOM. Nevertheless, it must be noted that the applied DVR has a 3 kVA rating which is very smaller compared to the DSTATCOM rating.

### *4.5.4 Stochastic Analysis Results*

Now, the stochastic analysis explained in Sect. 4.2 is carried out. In this case, first, let us assume that a DSTATCOM is installed at 2/3rd distance of feeder beginning. Voltage imbalance is only calculated at the end of the feeder since it was seen that it has its highest value at this point. The PDF of voltage imbalance at feeder end is

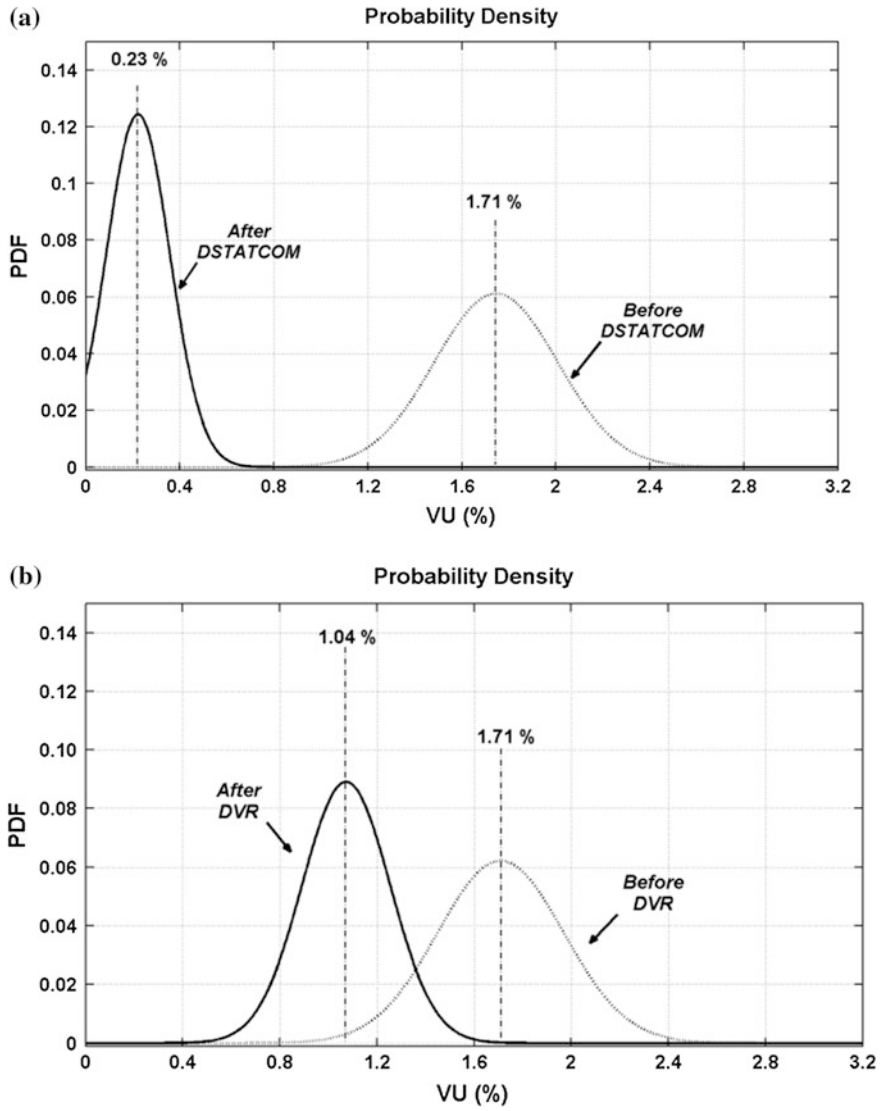


**Fig. 4.12** **a** Comparing PDF of voltage imbalance at feeder end before and after DSTATCOM installation, **b** Comparing PDF of highest voltage imbalance all along the feeder before and after DVR installation

shown in Fig. 4.12a. In this figure, the dashed line represents PDF before DSTATCOM installation and the solid line represents PDF after DSTATCOM installation. The average value of voltage imbalance at feeder end has reduced from 1.71 to 0.23 %. On the other hand, the probability of voltage imbalance at feeder end to be more than 2 % standard limit is reduced from 33.5 % to zero with the DSTATCOM is installed.

Now, let us assume that instead of DSTATCOM, a DVR is installed at 1/3rd distance of feeder beginning. Maximum of voltage imbalance is calculated all along the feeder. PDF of highest voltage imbalance is shown in Fig. 4.12b. In this figure, the dashed line represents PDF before DVR installation and the solid line represents PDF after DVR installation. The average value of highest voltage imbalance along the feeder has reduced from 1.71 to 1.04 %. On the other hand, the probability of voltage imbalance at feeder end to be more than 2 % standard limit is reduced from 33.5 % to zero with the DVR is installed. Comparing this figure with Fig. 4.12a, it is shown that DSTATCOM has better results in voltage imbalance reduction.

## 4.6 Application of CPDs: Dynamic Performance

The efficacy of the proposed CPDs in voltage imbalance reduction and voltage profile improvement was verified through steady–state load flow and stochastic analyses in the previous section. Although voltage imbalance and voltage regulation are predominantly steady–state (or quasi steady–state) issues, however, the dynamic characteristics of the proposed methods should also be investigated. It must be verified that these CPDs and their control strategies do not lead to instability in the system. In addition, it must be verified that they can respond effectively and promptly to load demand and PV output variations. This has been investigated through several case studies in PSCAD/EMTDC. Several studies are performed, some of which discussed below [25].

Let us assume that initially the total power generation of rooftop PVs are 40, 5 and 1 kW in phases *A*, *B* and *C*, respectively, while the loads in these phases are 20, 40 and 60 kW, respectively.

### *4.6.1 DSTATCOM Application*

Now, let us assume a DSTATCOM is installed at the 2/3rd point of the feeder, however it is not connected to the feeder. Then at $t = 1$ s the DSTATCOM is connected to the network. The PCC instantaneous and RMS voltages are shown in Fig. 4.13a and b. It can be seen from these figures that the three–phase voltage waveform seems more balanced and the RMS values of the three phases are shifted up close to the desired value ($E_{DSTAT} = 0.98$ pu).

With the system operating in the steady state, with the DSTATCOM being connected, the PV generation is increased by 13 and 1 kW in phases *A* and *B*, respectively at $t_1 = 0.05$ s. Subsequently at $t_2 = 0.35$ s, a load change is created in the network. A total 4 kW load is reduced from phase *A*, 8 kW increased in Phase *B* and 12 kW increased in phase *C*. Furthermore at $t_3 = 0.55$ s, another PV generation and load variation occur. A total 8 kW of PV output is reduced from

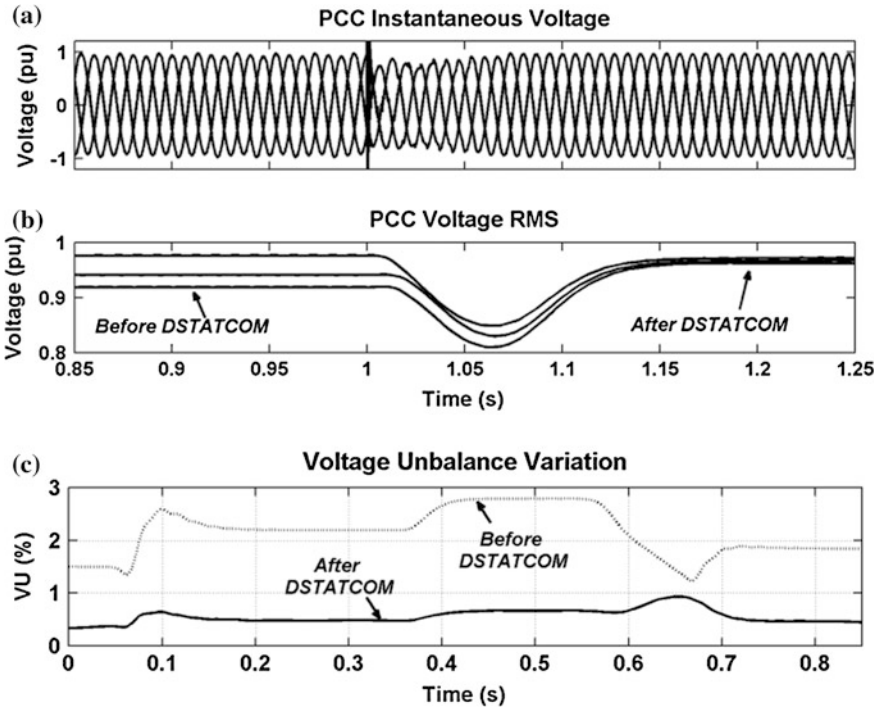


**Fig. 4.13** **a** PCC instantaneous voltage before and after DSTATCOM connection, **b** RMS voltage of PCC before and after DSTATCOM connection, **c** Voltage imbalance variation at low voltage feeder end before and after DSTATCOM installation

phase *A* while 2 kW and 6 kW PV output is increased in phases *B* and *C*, respectively. At the same time, the load in phase *A* in increased by 2 kW while the load in phases *B* and *C* is decreased by 4 and 6 kW, respectively.

The variation in voltage imbalance at the feeder end before and after DSTATCOM installation is shown in Fig. 4.13c. Comparing the voltage imbalance results in this figure, the efficacy of DSTATCOM application is verified. As seen from this figure, the DSTATCOM will vary the amount of its injected reactive power to the network based on network load and power parameters to fix the PCC voltage magnitude to the desired value.

### *4.6.2 DVR Application*

A similar study is carried out to investigate DVR dynamic performance. Let us assume a DVR is installed at 1/3rd point along the feeder. In Fig. 4.14a and b, the PCC instantaneous and RMS voltages are shown for cases before and after DVR connection. As it can be seen from these figures, the three–phase voltage

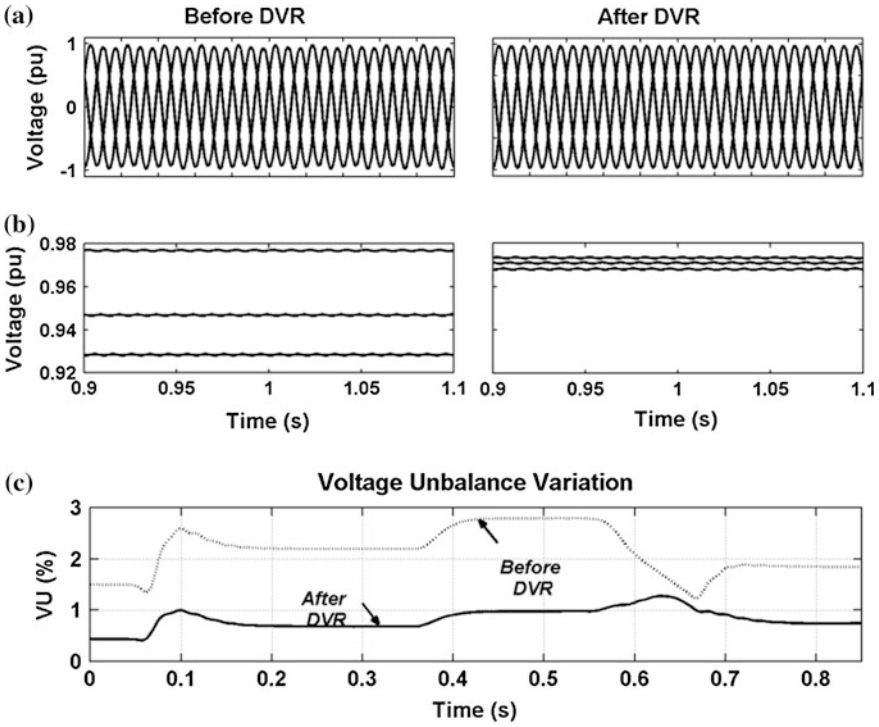


**Fig. 4.14** **a** PCC instantaneous voltage before and after DVR application, **b** PCC voltage RMS before and after DVR application, **c** Voltage imbalance variation at low voltage feeder end before and after DVR installation

waveform seems more balanced and the RMS values of the three phases are shifted up to the desired value of $E_{DVR} = 0.975$ pu.

The voltage imbalance at the end of the network before and after DVR installation is shown in Fig. 4.14c for the same PV generation and load variation discussed in the previous sub–section.

## 4.7 Conclusions

Random location and rating of single–phase rooftop PVs installed by householders may result in high voltage imbalance in low voltage feeders especially at far end nodes. For investigating this issue, a voltage imbalance sensitivity analysis and stochastic evaluation based on the rating and location of single–phase grid–connected rooftop PVs in a residential low voltage distribution network were presented in this chapter. Through the studies, it is proved that rooftop PV installation will have minor effect on the voltage imbalance at the beginning of a low voltage

feeder designed with engineering judgments. However, it might increase at the end of the feeder to more than the standard limit. It is also proved that depending on the load of the phase in which the PV is installed, the voltage imbalance will increase or decrease based on the location and rating of the PVs. The stochastic simulation demonstrated that the failure index of non–standard voltage imbalance in these networks is high (30.19 %). Later, the applications of DSTATCOM and DVR were investigated for voltage imbalance reduction. Based on numerical analyses in steady–state condition, it was shown that a DSTATCOM has better results for voltage profile improvement and voltage imbalance reduction in comparison with a DVR. The Monte Carlo based stochastic analyses proved that for any random load and PV rating and location scenarios, the discussed CPDs are successful in reducing voltage imbalance to below the standard limits.

## Appendix A

The stopping rule of the Monte Carlo method is chosen based on achieving an acceptable convergence for $\overline{VUF}$ and *Var(VUF)*. In this study, the program was rerun for several trial numbers. The mean ($\lambda$) and *Var(VUF)* at the beginning and end of feeder in addition to Failure Index ($F_I$ %)for different trial numbers is listed in Table A.1. From this table, it can be seen that the mean, variance and failure index values do not vary much after N = 10,000 trials. The error value in *Var(-VUF)* is given in the last column of the table assuming the base case of 10,000 trials. It can be seen that an increase in trial number from 10,000 does not increase the error in variance significantly. Therefore this value is chosen as the stopping rule.

**Table A.1** Convergence of Monte Carlo method for different trial numbers

| N (Trial number) | 1,000 | 5,000 | 10,000 | 20,000 | 30,000 | 50,000 | 75,000 | 100,000 |
|---|---|---|---|---|---|---|---|---|
| Failure index (*FI*) (%) | 4.9 | 4.34 | 6.89 | 6.99 | 7.03 | 7.07 | 6.96 | 7.00 |
| $\lambda$ at beginning of feeder | 0.38 | 0.38 | 0.38 | 0.38 | 0.38 | 0.38 | 0.38 | 0.38 |
| $\lambda$ at end of feeder | 1.54 | 1.53 | 1.53 | 1.53 | 1.53 | 1.53 | 1.53 | 1.53 |
| *Var(VUF)* at beginning of the feeder (%) | 0.16 | 0.17 | 0.19 | 0.18 | 0.19 | 0.18 | 0.18 | 0.18 |
| *Var(VUF)* at the end of feeder (%) | 5.92 | 6.0554 | 8.04 | 7.95 | 8.01 | 8.12 | 8.07 | 8.05 |
| Error (%) of end *Var (VUF)* to other trial numbers | 26.28 | 24.71 | 0 | 1.12 | 0.32 | 0.98 | 0.39 | 0.15 |

## Appendix B

The technical parameters of the considered network within the chapter are provided below (Table B.1).

**Table B.1** Technical parameters of the studied low voltage distribution network

| | |
|---|---|
| Transformer | 11 kV/415 V, 250 kVA, $\Delta/Y_{grounded}$, $Z_I = 4$ % |
| Feeder | $3 \times 70 + 35$ mm$^2$AAC overhead line for low voltage feeder, $3 \times 50$ mm$^2$ ACSR, 2 km overhead line |
| Rooftop PV | 1–5 kW, unity power factor, $L = 5$ mH |
| Loads | 1 kW, $\cos\varphi = 0.95$, $z = 51.9840 + \mathrm{j} \times 17.0863\ \Omega$<br>2 kW, $\cos\varphi = 0.95$, $z = 25.9920 + \mathrm{j} \times 8.5432\ \Omega$<br>3 kW, $\cos\varphi = 0.95$, $z = 17.3280 + \mathrm{j} \times 5.6954\ \Omega$ |
| PV location | 1 kW PV at node 7 of phase *A* and node 9 of phase *C*<br>2 kW PV at nodes 1 (2 PVs), 6 (2 PVs), 9 (2 PVs), 10 (2 PVs) of phase *A* and node 1of phase *B*<br>3 kW PV at nodes 2 (2 PVs), 3 (2 PVs), 5 (2 PVs), 8 of phase *A* and node 4 of phase *B* |

## References

1. Ghosh A, Ledwich G (2002) Power quality enhancement using custom power devices. Kluwer Academic Publishers, Boston
2. Short TA (2004) Electric power distribution handbook. CRC Press, Boca Raton
3. Jouanne AV, Banerjee B (2001) Assessment of voltage imbalance. IEEE Trans Power Delivery 16(4):782–790
4. Gnacinski P (2008) Windings temperature and loss of life of an induction machine under voltage unbalance combined with over—or undervoltages. IEEE Trans Energy Convers 23(2):363–371
5. International Energy Agency (IEA) (2008) PVPS annual report—implementing agreement on photovoltaic power systems,—photovoltaic power systems programme
6. Eltawil MA, Zhao Z (2010) Grid–connected photovoltaic power systems: technical and potential problems—a review. Renew Sustain Energy Rev 14(1):112–129
7. Papathanassiou SA (2007) A technical evaluation framework for the connection of DG to the distribution network. Electr Power Syst Res 77:24–34
8. Lopes JAP, Hatziargyriou N, Mutale J, Djapic P, Jenkins N (2007) Integrating distributed generation into electric power systems: a review of drivers, challenges and opportunities. Electr Power Syst Res 77:1189–1203
9. Shahnia F, Majumder R, Ghosh A, Ledwich G, Zare F (2010) Sensitivity analysis of voltage imbalance in distribution networks with rooftop PVs. IEEE Power Energy Soc Gen Meet 80:1–8
10. Li W (2005) Risk assessment of power systems: models, methods, and applications. Wiley Publishers, New york
11. Shahnia F, Majumder R, Ghosh A, Ledwich G, Zare F (2011) Voltage imbalance analysis in residential low voltage distribution networks with rooftop PVs. Electr Power Syst Res 81(9):1805–1814

12. Mazumder S, Ghosh A, Shahnia F, Zare F, Ledwich G (2012) Excess power circulation in distribution networks containing distributed energy resources. IEEE Power Energy Soc Gen Meet, 1–8
13. Shahnia F, Ghosh A, Ledwich G, Zare F (2012) An approach for current balancing in distribution networks with rooftop PVs. IEEE Power Energy Soc Gen Meet, 1–6
14. Shahnia F, Wolfs P, Ghosh A (2013) Voltage unbalance reduction in low voltage feeders by dynamic switching of residential customers among three phases. IEEE Power Energy Soc Gen Meet, 1–5
15. Ghosh A (2005) Performance study of two different compensating devices in a custom power park. IEE Gener Transm Distrib 152(4):521–528
16. Australian Standard Voltage, AS60038–2000
17. IEEE recommended practice for monitoring electric power quality, IEEE Standard 1159–1995
18. Planning Limits for Voltage Unbalance in the United Kingdom (1990) The Electricity Council, Engineering Recommendation P29
19. Lee K, Venkataramanan G, Jahns T (2006) Source current harmonic analysis of adjustable speed drives under input voltage unbalance and sag conditions. IEEE Trans Power Delivery 21(2):567–576
20. Valois PVS, Tahan CMV, Kagan N, Arango H (2001) Voltage unbalance in low voltage distribution networks. In: Proceeding of 16th International Conference on Electricity Distribution (CIRED)
21. Power quality measurement results in 120 points in Eastern Azarbayjan Electric Power Distribution Co., Technical report, 2008 (in Persian)
22. IEEE Standard 929–2000. IEEE recommended practice for utility interface of photovoltaic (PV) systems
23. Makrides G, Zinsser B, Norton M, Georghiou GE, Schubert M, Werner JH (2010) Potential of photovoltaic systems in countries with high solar irradiation. Renew Sustain Energy Rev 14:754–762
24. Parker D, Mazzara M, Sherwin J (1996) Monitored energy use patterns in low–income housing in a hot and humid climate. In: Proceeding of 10th symposium on improving building systems in hot humid climates
25. Shahnia F, Ghosh A, Ledwich G, Zare F (2011) Voltage correction in low voltage distribution networks with rooftop PVs using custom power devices. In: 37th Annual Conference on IEEE Industrial Electronics Society (IECON), pp 991–996, Nov 2011
26. Shahnia F, Ghosh A, Ledwich G, Zare F (2010) Voltage unbalance reduction in low voltage distribution networks with rooftop PVs. In: 20th Australasian universities power engineering conference (AUPEC), pp. 1–5, Dec 2010